Article

Green Biobased Polyethylene Terephthalate (bioPET) Composites Reinforced with Different Lengths of Basalt Fiber for Technical Applications

Stanisław Kuciel *[ID] and Karina Rusin-Żurek

Department of Materials Engineering, Faculty of Materials Engineering and Physics, Cracow University of Technology, Warszawska 24, 31-155 Cracow, Poland; karina.rusin-zurek@pk.edu.pl
* Correspondence: stanislaw.kuciel@pk.edu.pl

Abstract: This paper presents the modification results and effects of reinforcing green polyethylene terephthalate matrix composites (bioPET ECOZEN® T120) with basalt fibers of two different lengths. Five types of composites with two filling levels of 7.5 and 15 wt% of each fiber were produced by injection molding. Basic mechanical and processing properties, microstructure photographs, and reinforcement effects were analyzed and low- and high-cycle fatigue tests were performed. A significant increase in strength and stiffness was observed (especially for short fibers) proportional to the amount of fibers; longer fibers would also increase the deformation capacity of the composite. Furthermore, longer fibers would reduce relaxation processes (creep) but would not increase the dissipation capacity and mechanical energy. Predictability of fatigue effects enables optimal environmentally friendly materials to be designed.

Keywords: PET; basalt fibers; composites; fatigue test; mechanical properties

1. Introduction

Growing environmental concerns and the depletion of fossil resources have intensified the search for sustainable and eco-friendly materials [1]. Among these sustainable materials, green biobased polyethylene terephthalate (bioPET) has emerged as a promising alternative to conventional PET, which is derived from non-renewable fossil fuels [2,3]. BioPET is produced from renewable resources such as plant-derived ethylene glycol and offers similar mechanical properties, processability, and recyclability to its petroleum-based counterpart but with a reduced carbon footprint, making it a favorable candidate for sustainable material applications [4–6].

In order to improve the mechanical and thermal properties of polymers, additives in the form of reinforcing fibers are often used. Fibers such as glass, carbon, or aramid are commonly used to reinforce traditional plastics, enhancing their strength, stiffness, and resistance to high temperatures [7–9]. The addition of fibers not only improves the mechanical properties of the material but also affects its durability and performance in engineering applications [10,11]. One type of fiber used to reinforce polymers is basalt fiber. Basalt fibers, derived from natural volcanic basalt rock, have gained attention due to their excellent mechanical properties, high thermal stability, and resistance to chemical and environmental degradation [12–14]. These fibers are produced through the melting and extrusion of basalt rocks at high temperatures, resulting in continuous fibers that can be used as reinforcement in polymer composites [15]. The inherent properties of basalt fibers, such as high tensile strength, modulus, and thermal stability, make them suitable for reinforcing polymers, thus enhancing the overall performance of the composite material [16–18]. Basalt fibers offer several significant advantages compared to glass and carbon fibers. Firstly, basalt fibers exhibit higher tensile strength and better resistance to high temperatures than glass fibers [19,20]. In comparison to carbon fibers, basalt

fibers are more cost-effective, making them a more economical choice for many industrial applications [21]. Additionally, basalt fibers are less prone to chemical corrosion and have better resistance to aggressive environments, which enhances their durability and reliability under harsh operating conditions [22].

Combining bioPET with basalt fibers leads to the development of composites that harness the benefits of both materials: the sustainability and recyclability of bioPET and the superior mechanical and thermal properties of basalt fibers. These composites have the potential to replace conventional materials in various technical applications, including automotive parts, construction materials, and electronic housings [23]. Moreover, basalt fibers are naturally abundant and non-toxic, aligning with the increasing demand for environmentally benign and sustainable materials [24]. There are few scientific articles on biobased PET, and only a handful specifically address PET reinforced with basalt fibers. For instance, researchers investigated the mechanical and thermal properties of PET/basalt fiber composites, finding significant improvements in tensile and flexural strength, impact resistance, and thermal stability compared to neat PET. In the study [25], pellets from recycled PET (rPET) obtained from milled beverage bottles were used. Short glass fibers (GF) and short basalt fibers (BF) (with an average length of 1.1 mm and a diameter of 10.0 μm) were employed as reinforcements. Composites of 15%, 30%, and 45% by weight were produced using injection molding. Both glass and basalt fibers significantly improved the stiffness of the composites. At a 45% basalt fiber content, the Young's modulus values increased by 100%, bending strength by 40%, and bending modulus by 200%. However, despite achieving reinforcement, the authors noted a need to improve compatibility and adhesion with the PET matrix. For this purpose, fibers are often coated with a coupling agent, usually silanes, which improves adhesion by chemically bonding to both the polymer and the fiber surface [26–28]. In [29], a composite produced from recycled PET was reinforced with basalt fiber at 20% and 30% by weight (with an average length of 4 mm and a diameter of 15 μm). The composites were produced using a twin-screw extruder. SEM images showed a high level of fiber dispersion and homogenous distribution within the polymer matrix, but weak adhesion. Increasing the fiber content from 20% to 30% did not lead to fiber agglomeration, and the dispersed structure was maintained. Improved adhesion was achieved only after adding talc. In terms of mechanical properties, the best reinforcement was obtained in the composites with 30% fiber content and the addition of talc. In another study [30], the effect of adding short basalt fibers as reinforcement for polypropylene and the effect of fiber size on adhesion and resulting mechanical properties were investigated. The fiber contents were 10%, 20%, and 30% by weight. The results demonstrated that the properties of polypropylene improved in both tensile and bending tests. Specifically, tensile strength increased by 64% and Young's modulus by 110% with the addition of short basalt fibers. These parameter values increased with higher fiber content.

The mechanical improvement resulting from short fiber reinforcement is mainly dependent on factors such as fiber content, fiber length, orientation and fiber–matrix adhesion [31,32]. Short fibers are generally easier to process and distribute uniformly within the matrix but may not provide the same level of mechanical enhancement as long fibers [33]. Conversely, long fibers can significantly improve the tensile strength, impact resistance, and overall toughness of the composite but may pose challenges in terms of processing and dispersion [34]. Understanding the optimal fiber length for specific applications is crucial for tailoring the properties of polymer/basalt fiber composites to meet the desired performance criteria. Arslan et al. [35] investigated the effect of the amount of basalt fiber (BF) and initial fiber length on the tensile, flexural and impact properties of poly (butylene terephthalate) (PBT)-based composites. BF was used in amounts of 5, 10, 20 and 30% by weight with different initial lengths of 3, 6 and 12 mm at constant BF loading (20% by weight). The components of the composites were mixed using a co-rotating twin screw extruder and then produced using injection molding. Tests showed that the addition of BF improved the tensile strength and thermal stability of PBT at 20 and 30 wt% addition. Flexural strength and elastic modulus increased with increasing added amount of BF,

reaching the best results at 30% BF addition. At an addition of 20% by weight, the effect of fiber lengths of 3, 6 and 12mm was analyzed, reaching the highest strength increases for fiber lengths of 6 mm. Compared to neat PBT, tensile strength increased by 16%, flexural strength by 74% and flexural modulus by 166%. In another study [36], basalt fibers of 3 and 12 mm length were added to polyamide 6.6 at 23 and 30% by weight. The tests showed that the length of the fibers had a greater effect on the mechanical properties of the composites than their percentage by weight. Composites with 12 mm basalt fibers at 23% and 30% by weight had higher tensile strength and modulus than composites with 3 mm basalt fibers, while composites with 3 mm basalt fibers at 30% by weight resulted in a 25% increase in flexural strength. Similarly, [37] showed that the length of basalt fibers has a significant effect on the mechanical properties of composites obtaining the best results for a fiber length of 10 mm.

The focus of this study is the development and characterization of bioPET composites reinforced with basalt fibers of different lengths. The aim is to understand how the length of basalt fibers influences the mechanical and fatigue properties and overall performance of the bioPET composites. This research is important for optimizing material properties for specific technical applications and developing the use of sustainable materials in the engineering and industrial sectors. Our paper investigates for the first time the effect of fiber length on a biobased PET matrix and presents an original method for evaluating energy dissipation changes in the first loops of mechanical hysteresis.

2. Materials and Methods

2.1. Material and Composite Preparation

As a matrix bio-based polyethylene terephthalate (bioPET ECOZEN T120) from SK Chemicals (Seongnam-si, Republic of Korea) was used. This polymer is a glycol-modified polyethylene terephthalate (PETG) with 15% plant-derived biomass components and has the following properties: density 1.27 g/cm^3, tensile strength 51 MPa, flexural strength 76 MPa, flexural modulus 1800 MPa, and Izod notched impact strength of 93 kJ/m^2. According to the manufacturer's data, this polymer does not contain bisphenol derivatives (BPA, etc.) or phthalate-based plasticizer ingredients. Before processing, bioPET pellets were dried in a molecular dryer at 90 °C for 6 h. In order to produce composites, the following additives were added to the matrix:

Short and long basalt fibers (KV02M and KV16) produced by Basaltex (Wevelgem, Belgium); properties: density 2.67 kg/dm^3, Young's modulus 93–110 GPa, tensile strength 4150–4800 MPa; sizing type: silane

(1)   BCS 13–3.2—KV02M with diameter 13 µm, cut length 3.2 mm (short fibers),
(2)   BCS 17–6.4—KV16 with diameter 17 µm, cut length 6.4 mm (long fibers)

Composite pellets were produced using a compounding line with a Steer Omega 20H (Bangalore, India) co-rotating twin-screw laboratory extruder (D = 20 mm, L/D = 44). The process was carried out at 260 °C, and the screw speed was set to 90 rpm. In the granulating machine used, basalt fibers were added via gravimetric dispensers, allowing the fiber content of the composite to be accurately determined. A long 8-cylinder mixing zone using variable geometry screws enabled thorough mixing.

Standard samples were produced by injection molding (KM 40-125 Winner Krauss Maffei, Krauss Maffei, Munich, Germany) according to the PN-EN ISO:3167 standard [38]. On this bioPET matrix, five composites were produced containing 7.5 and 15% basalt fibers by weight. The parameters of the injection process were temperatures in the zones: 180, 285, 290, 290, and 295 °C and injection pressure: 1000 bar, and were the same for all composites. The produced composites and their abbreviations and densities are presented in Table 1.

Table 1. Abbreviations and densities of the bioPET composites with basalt fibers.

Samples	Compositions	Density [g/cm^3]
bioPET	bioPET Ecozen T120	1.252
bioPET + 7.5 SB	bioPET + 7.5% short basalt fibers	1.317
bioPET + 7.5 LB	bioPET + 7.5% long basalt fibers	1.305
bioPET + 15 SB	bioPET + 15% short basalt fibers	1.350
bioPET + 15 LB	bioPET + 15% long basalt fibers	1.346

2.2. Testing Methods

2.2.1. Scanning Electron Microscopy (SEM)

To evaluate the adhesion between the basalt fibers and the polymer matrix, as well as the morphology of the composite surface at fractures after tensile testing, SEM micrographs were performed using a scanning electron microscope SEM (JEOL JSM-IT200, Tokyo, Japan) in low vacuum at 5 kV at 250× and 500× magnification. Before placing the composites in the electron microscope chamber, they were covered with gold particles using a sputter coater (DII-29030SCTR, JEOL, Tokyo, Japan).

2.2.2. Mechanical and Fatigue Tests

The density of the composites was determined by the hydrostatic method using a RADWAG WAS 22W analytical balance (Radwag, Radom, Poland) according to PN-EN ISO 1183 [39]. Ethanol was used as a reference liquid. For all measurements, at least three samples were measured and average values were recorded.

The static tensile tests and low-cycle dynamic tests were conducted using a Shimadzu AGS-X 10 kN (Kyoto, Japan) testing machine. Tensile testing was carried out in accordance with the PN-EN ISO 527 standard [40]. The crosshead speed was 10 mm/min. In order to determine the mechanical hysteresis loop, the test used cyclic force loading from a minimum value of 200 N to a maximum value of 1800 N and displacement changes were observed. The speed was 100 mm/min, which is equivalent to a low frequency of cycling and allows for the visualization of viscous phenomena. The three-point bending tests were performed on an MTS Criterion 43 (Eden Prairie, MN, USA) universal testing machine with MTS software TestSuites 1.0 in accordance with the PN-EN ISO 178 standard [41]. The crosshead speed was 10 mm/min. The impact tests were carried out using the Charpy method on a Zwick/Roell MTS-SP testing machine (Ulm, Germany), in accordance with the PN-EN ISO 179 standard [42]. The samples were unnotched. The impact energy was 2 and 5 J.

High-cyclic fatigue tests were performed under stress-controlled tension–tension conditions using a Shimadzu Servopulser EMT (Kyoto, Japan) hydraulic tensile machine at a 1 Hz cyclic frequency with a sinusoidal waveform. The testing program Data Viewer for 4830 consisted of several cyclic load blocks. The maximum force in the first block was selected in proportion to the maximum static force, starting from 30% of the maximum force for each degree of sample infill. For each subsequent load block containing 1000 cycles, starting with a force of 700 N and increasing by 400 N, respectively: cycle 1—0.7–1.1 kN, cycle 2—0.7–1.5 kN, cycle 3—0.7–1.9 kN, cycle 4—0.7–2.3 kN. Mechanical hysteresis loops were recorded and the dissipation energy was calculated for the last loop from each load block.

2.2.3. Contact Angle and Total Surface Free Energy by the Owens–Wendt Method

Before testing, the samples were thoroughly cleaned with isopropanol and then dried at room temperature for 24 h. Contact angle and surface free energy were measured using a goniometer (See System 7.0, Advex Instruments, Czech Republic) on the surface of the composites. Water and diiodomethane were used as measuring liquids. Liquid droplets of 5 μL were applied to the surface of the samples using an automatic pipette. The wetting

angle was measured for each sample at three different points to obtain reliable values. Each measurement was repeated three times for each measuring liquid to increase the accuracy of the results. The Owens–Wendt method was used to calculate the surface free energy of the composite materials. This is a widely used technique for determining the surface free energy (SFE) of solid materials. This method divides surface energy into two main components: the dispersive component, related to van der Waals forces, and the polar component, associated with dipole interactions and hydrogen bonding. To apply the method, contact angles of at least two liquids with known surface tension properties are measured on the solid's surface. These measurements are then used to calculate the material's polar and dispersive components, providing insight into its wettability and adhesive properties [43,44]. See System 7.6 software provided the results to calculate the surface free energy, based on the equation:

$$\gamma_s = \gamma_s^d + \gamma_s^p \tag{1}$$

where:

γ_s—total surface free energy,

γ_s^d—the dispersive component of the surface free energy,

γ_s^p—the polar component of the surface free energy.

3. Results and Discussion

3.1. Scanning Electron Microscope (SEM) Micrographs

Figure 1 shows SEM micrographs at 250× and 500× magnification of the sample surfaces after tensile testing of bioPET composites with the addition of short and long basalt fibers.
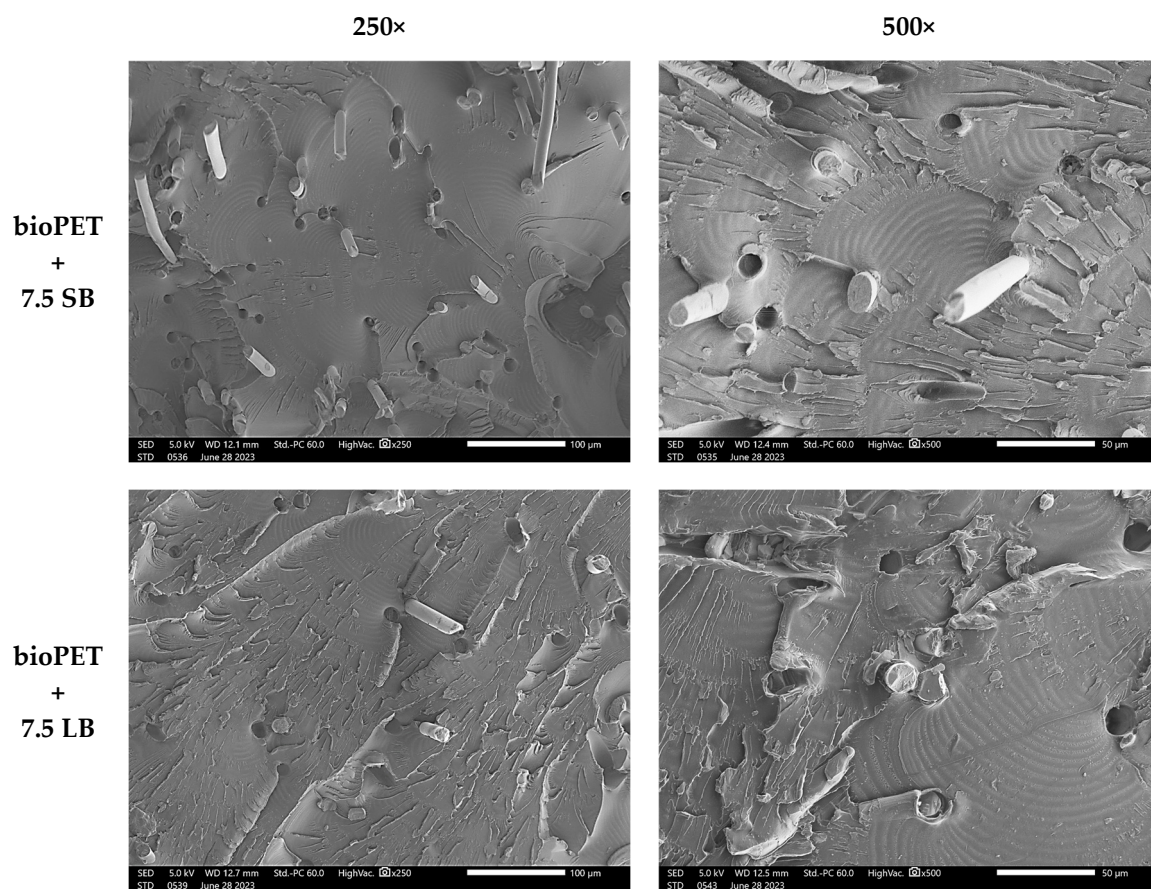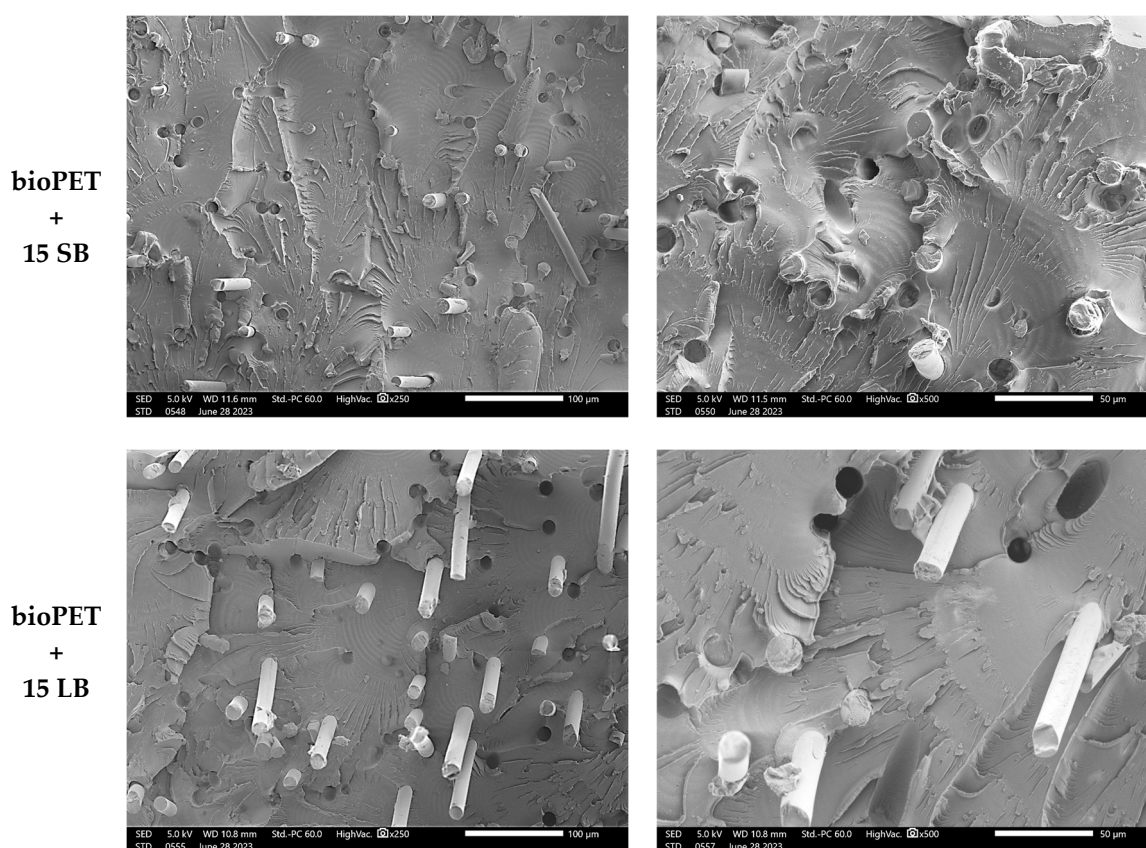

Figure 1. *Cont.*

Figure 1. SEM microphotographs of composites at 250× and 500× magnification.

At the fractures of the tensile samples, we observed basalt fibers distinctly well embedded in the polymer matrix in the background of crystalline groupings characteristic of polyethylene terephthalate surfaces. The basalt fibers show a diameter in accordance with the producer's data, i.e., 13 μm for short fibers and 17 μm for long fibers. Due to compauding, i.e., mixing of fibers in the plasticizing zone of the injection molding machine, long fibers break to a length of 150–200 μm and short fibers break to a maximum of 100 μm. The change in length and breaking of fibers during processing is common. In another study [25], after analyzing fiber lengths, a significant degradation in length during processing was also noted, from an initial length of 1.1 mm to approximately 60 μm after extrusion and injection molding. The fractures of composites with 15% of both short and long fibers are characterized by a mixed nature; apart from brittle fracture, fragments of ductile fracture can be observed due to the higher character of the reinforcement. In most fractures we observe characteristic symptoms of "pull out", i.e., pulling out of fibers from the polymer matrix reaching up to 40%, probably due to the lack of addition of a compatibilizer or limited fiber aperture capabilities.

3.2. Mechanical Properties

3.2.1. Static Tensile and Three-Point Bending Tests

The results for mechanical properties from the static tensile and three-point bending tests are compared in Table 2. Figure 2 presents static tensile curves of bioPET and its composites and Figure 3 a comparison of tensile strength and Young's modulus.

Analyzing the strength properties values from static tensile and three-point bending tests, it can be seen that the addition of basalt fibers significantly increases the tensile and flexural strengths and the modulus of elasticity, and significantly reduces the strain at break. The higher the basalt fiber content, the higher the values of these parameters.

Table 2. Results of tensile, bending and impact tests.

Samples	Tensile Test			Bending Test			Impact Strength [kJ/m^2]
	Tensile Strength [MPa]	Young's Modulus [MPa]	Strain at Break [%]	Bending Strength [MPa]	Flexural Modulus [MPa]	Max. Deflection [mm]	
bioPET	53.7 $\pm$ 0.5	2425 $\pm$ 133	78.2 $\pm$ 5.2	84.5 $\pm$ 0.4	2328 $\pm$ 79	>10	-
bioPET + 7.5 SB	75.4 $\pm$ 3.3	4396 $\pm$ 151	4.6 $\pm$ 0.1	102.7 $\pm$ 2	3117 $\pm$ 96	9.8 $\pm$ 0.3	23.1 $\pm$ 1.8
bioPET + 7.5 LB	67.8 $\pm$ 1.3	4315 $\pm$ 103	4.4 $\pm$ 0.1	94.7 $\pm$ 3.0	2705 $\pm$ 150	11.7 $\pm$ 0.5	20.2 $\pm$ 2.3
bioPET + 15 SB	84 $\pm$ 4.6	5987 $\pm$ 312	3.9 $\pm$ 0.2	120.9 $\pm$ 4.8	4142 $\pm$ 122	5.9 $\pm$ 0.2	32.3 $\pm$ 3.6
bioPET + 15 LB	75.9 $\pm$ 3.4	5402 $\pm$ 371	4 $\pm$ 0.2	106.9 $\pm$ 1.7	3599 $\pm$ 187	6.6 $\pm$ 0.4	28.1 $\pm$ 1.2
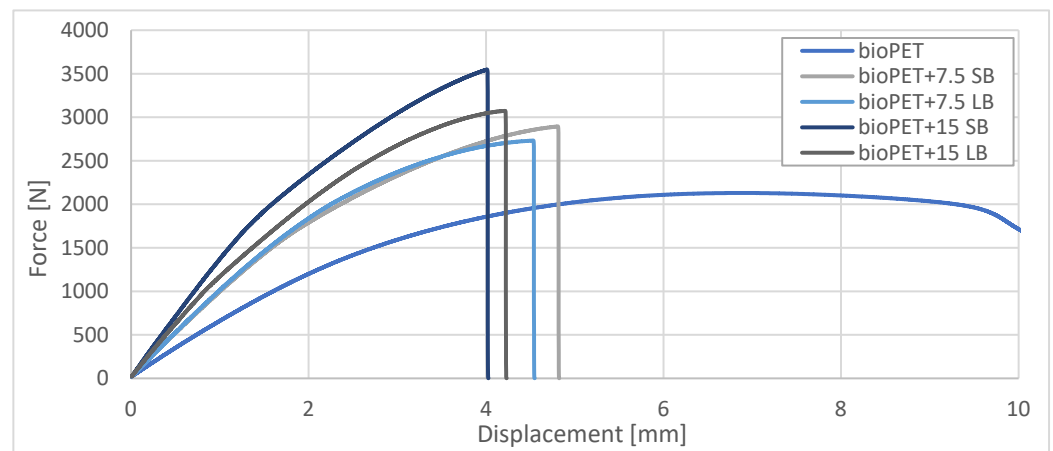
Figure 2. Static tensile curves of bioPET and its composites with basalt fibers.
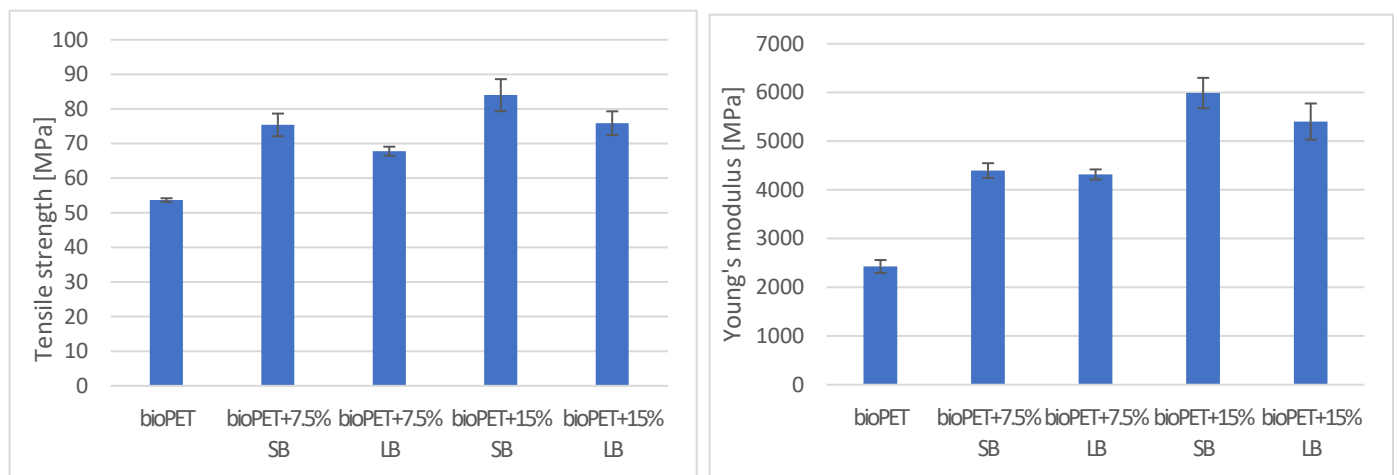
Figure 3. Comparison of tensile strength and Young's modulus of bioPET composites.

Short basalt fibers in bioPET composites show higher efficiency in improving impact strength compared to long fibers. Composites containing short basalt fibers show higher impact strength by about 15% compared to composites with long basalt fibers at the same fiber mass content. This may be due to better dispersion of short fibers in the polymer matrix, leading to better load transfer and prevention of crack propagation. Increasing the basalt fiber content from 7.5% to 15% leads to an increase in impact strength of about 40% for both short and long fibers. The highest impact strength was obtained for the bioPET

composite with 15% short basalt fibers (32.3 kJ/m²), indicating that this fiber configuration is most favorable for improving dynamic-type impact resistance.

Figure 4 presents three-point bending curves for bioPET and its composites. Comparisons of flexural strength and modulus are shown in Figure 5.
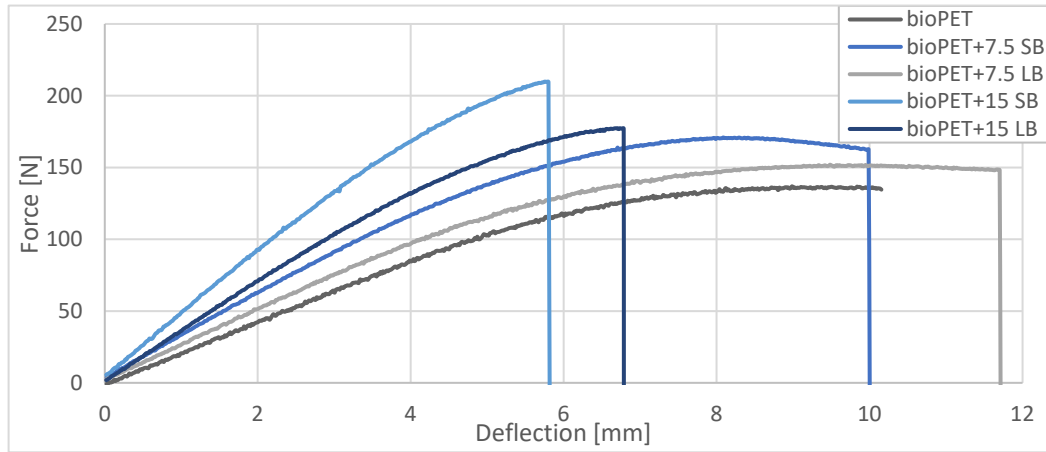

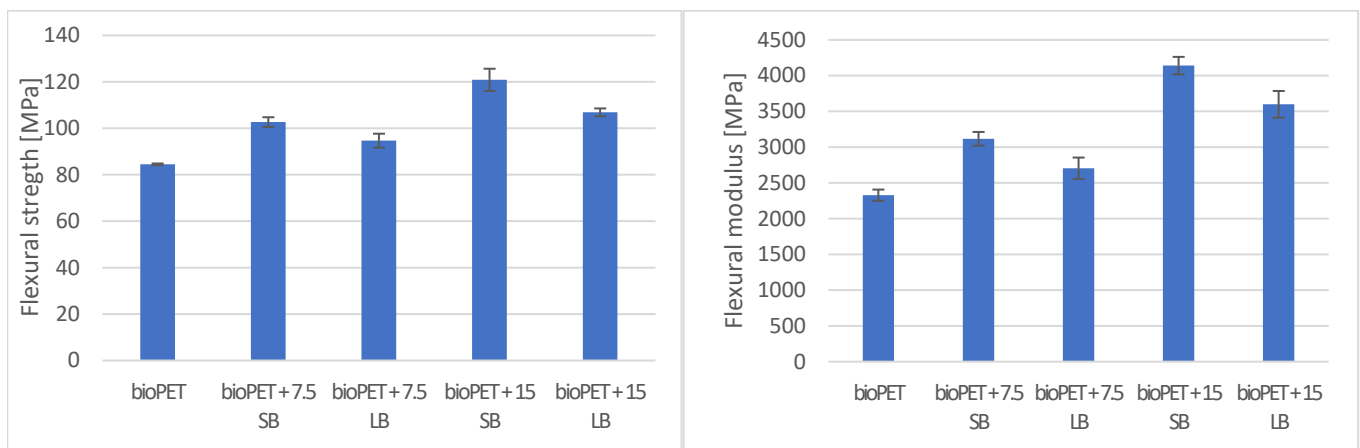**Figure 4.** Three-point bending curves of bioPET and its composites.

Figure 5. Comparison of flexural strength and flexural modulus of bioPET composites.

Analyzing the tensile and bending curves, we can observe that the addition of basalt fibers significantly increases the maximum force transferred during the test and makes the composites much stiffer, causing a reduction in the maximum deformation of the composites (by almost 20 times).

In both tests, the highest values were obtained for the composites with the addition of 15% short basalt fibers, and the lowest for those with 7.5% long fibers content. The addition of basalt fibers increased tensile strength by 26-41% and Young's modulus by 78–147%, causing almost 20 times less strain at break.

A similar correlation is noticeable in the bending test, where higher parameter values were also obtained for composites with the addition of short fibers. Bending strength and flexural modulus increased by 12–43% and 16–78%, respectively.

Short fibers reinforce bioPET composites better than long fibers. For the same fiber amount, we can note that short fibers, relative to long fibers, result in an increase in tensile parameters by about 10% and bending parameters by 8–15%.

In order to verify the experimental results of the Young's modulus values and the anisotropy of the composite, the theoretical Young's modulus was also calculated when the composite carries loads in the direction parallel or perpendicular to the fibers. Figure 6

shows a comparison of the experimental and theoretical values of Young's modulus depending on the volume proportion of basalt fibers. Calculations were made using the following formulas:

(1) Conversion of mass proportion to volume fraction of fibers:

$$V_f = \frac{1}{1 + \frac{\rho_f}{M_f \rho_m}\left(1 - MF_f\right)} \tag{2}$$

where:

V_f—fiber volume fraction
MF_f—fiber mass fraction
ρ_f—fiber density
ρ_m—matrix density

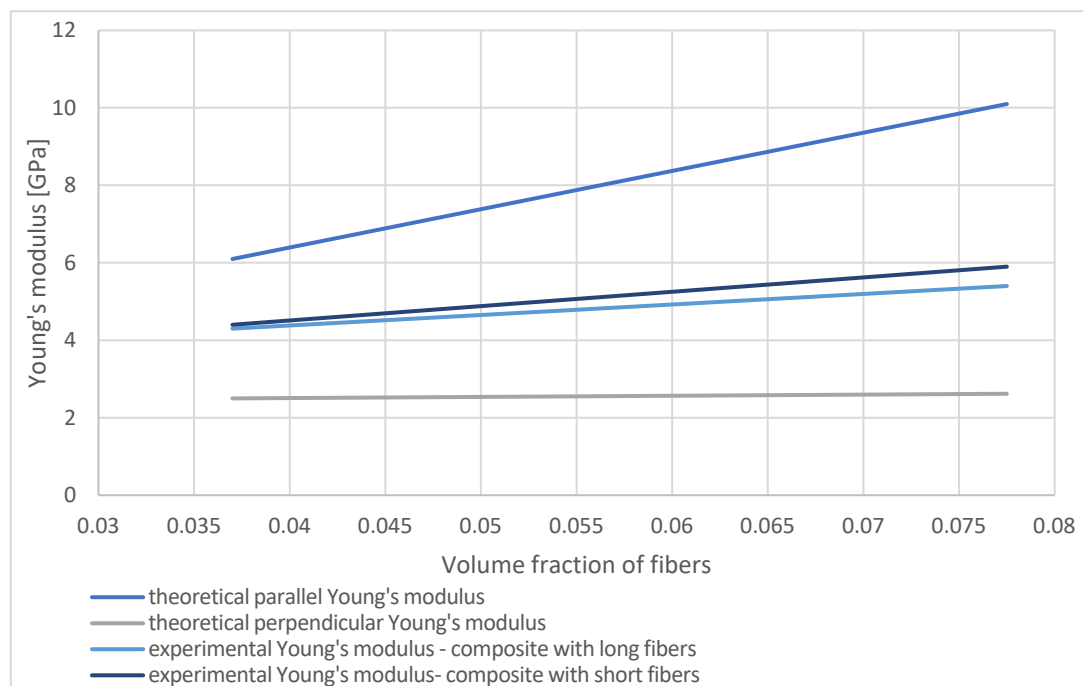(2) Theoretical Young's modulus when the composite carries loads in the direction parallel to the fibers

$$E_c = V_f E_f + \left(1 - V_f\right) E_m \tag{3}$$

where:

E_c, E_f E_m—composite, fiber, matrix Young's modulus

(3) Theoretical Young's modulus when the composite carries loads in the direction perpendicular to the fibers:

$$E_c = \frac{1}{\frac{V_f}{E_f} + \frac{1 - V_f}{E_m}} \tag{4}$$

Figure 6. Comparison of experimental and theoretical values of Young's modulus at load transfers parallel and perpendicular to the direction of basalt fiber placement, depending on their volume fraction.

The presented calculations indicate that the fibers are mostly aligned at different angles (significant mixing has occurred), and neither the perpendicular nor the parallel direction to the injection direction is dominant. Short fibers are more often aligned parallel to the injection direction than long fibers, which are more difficult to rotate.

3.2.2. Low Cycle Dynamic Test

Tests conducted under low-cycle kinematic loads were intended to determine how the produced composites behave during the first loading cycles, when the first relaxation processes and tendencies of the fibers to pull out of the matrix become apparent. The changes in the peak values of the hysteresis loops are most pronounced in the first few dozen cycles—which is why they were studied carefully for the first 20 cycles. After that, they tend toward a steady-state cycle. Another phenomenon is the accumulation of cyclic plastic deformation when the material is subjected to asymmetric stress cycles. This is the phenomenon of cyclic creep. Figures 7 and 8 show the mechanical hysteresis loops for cycles 1 and 20 for neat bioPET and its composites with the addition of 7.5% short and long basalt fibers. Figure 9 compares mechanical energy dissipation values between the 1st and 20th cycles.
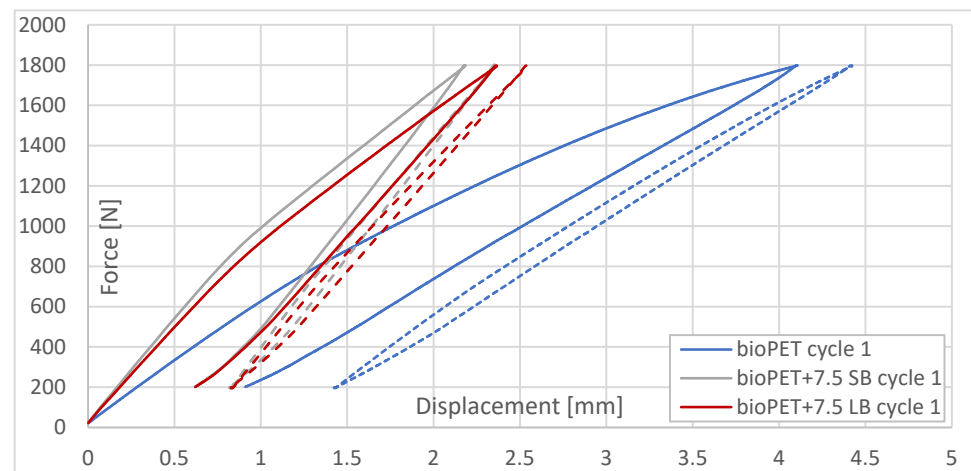
Figure 7. Comparison of energy dissipation loops for 1st and 20th cycles of neat bioPET and its composites with 7.5% basalt fibers (solid line—cycle 1, dashed line—cycle 20).
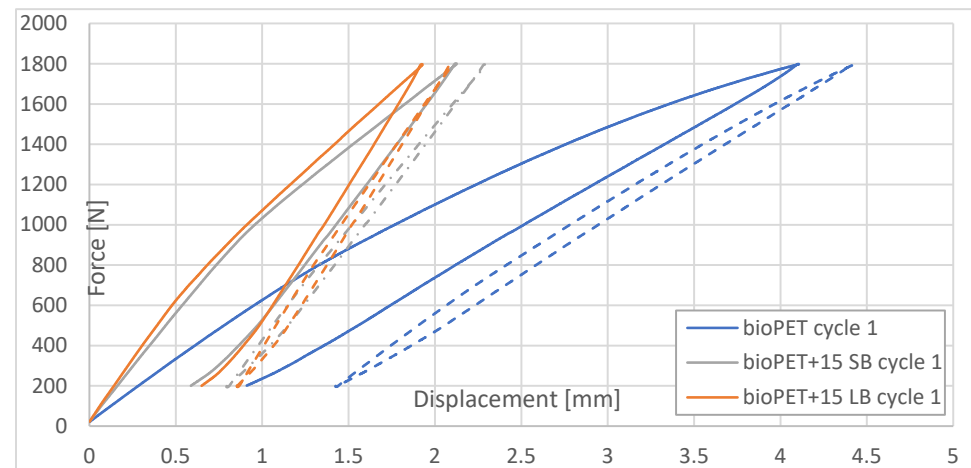
Figure 8. Comparison of energy dissipation loops for 1st and 20th cycles of neat bioPET and its composites with 15% basalt fibers (solid line—cycle 1, dashed line—cycle 20).

Composites with short basalt fibers at an addition of 7.5% by weight have the lowest mechanical energy dissipation capacity and high stiffness in the first 20 cycles of mechanical hysteresis.

Composites with 15 wt% long fiber content have the lowest mechanical energy dissipation capacity and high stiffness. Presumably, with a higher amount of long fibers by volume, the pulling forces of the long fibers from the matrix begin to clearly interact in favor of higher stiffness and lower mechanical energy dissipation capacity.

A comparison of the ability to dissipate mechanical energy indicates that it decreases with successive cycles of dynamic loading and the addition of more fibers. With increasing load cycles, composites with higher long fiber content have the lowest mechanical energy dissipation capacity and the highest stiffness.
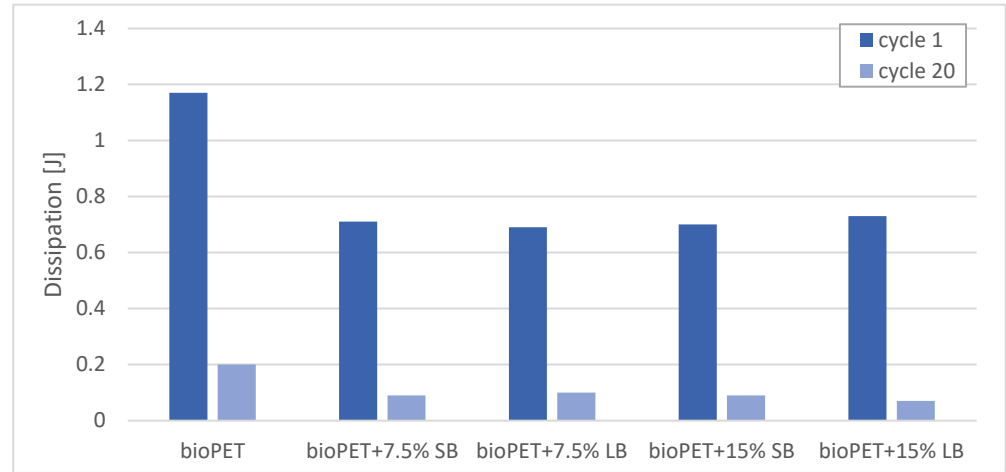

Figure 9. Comparison of energy dissipation between 1st and 20th cycles of bioPET and its composites.

3.2.3. High Cycle Dynamic Test

The phenomenon of cyclic deformation under dynamic forcing (with load ranges beginning from 0.7 kN and increasing by 0.4 kN after every 1000 cycles) is shown in Figures 10–14 for neat bio-polyethylene terephthalate and its composites. Under the test conditions of constant stress over the entire range of successive cycles, the material experiences weakening when strain amplitudes increase and conversely experiences strengthening when strain amplitudes decrease. Figure 15 shows the maximum displacement in the loop for neat bioPET and its composites in each block of load cycles.
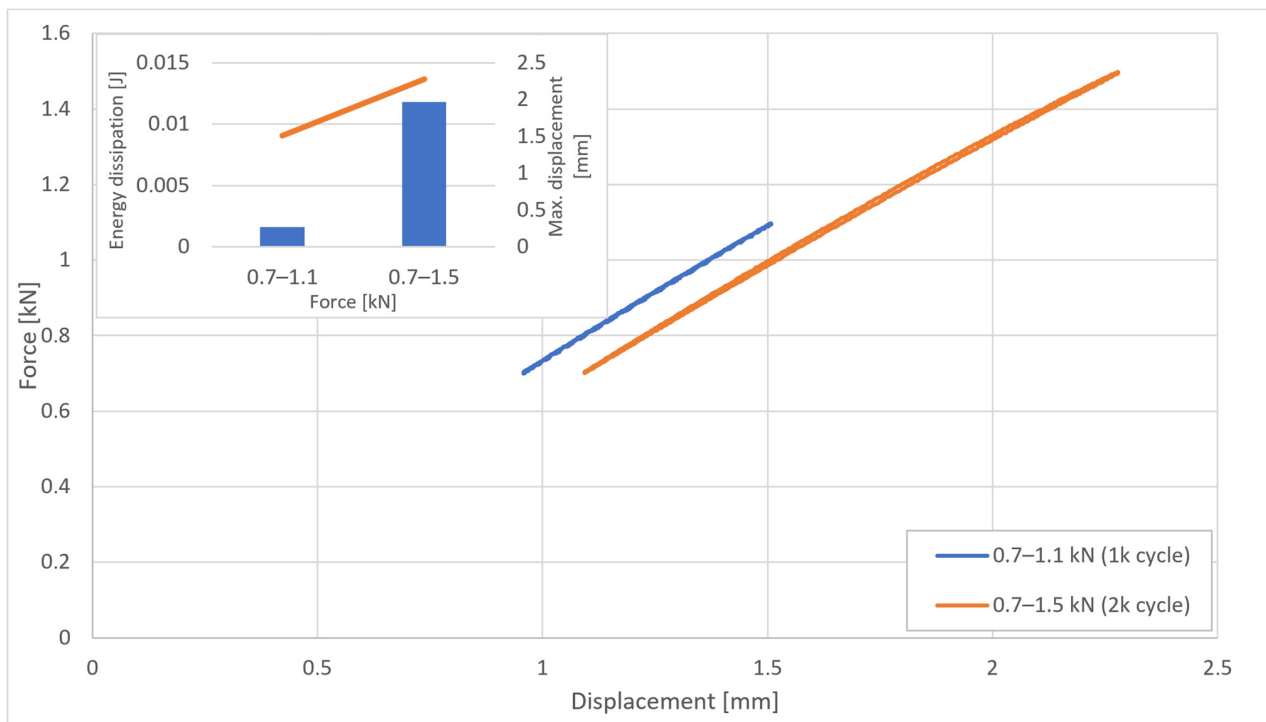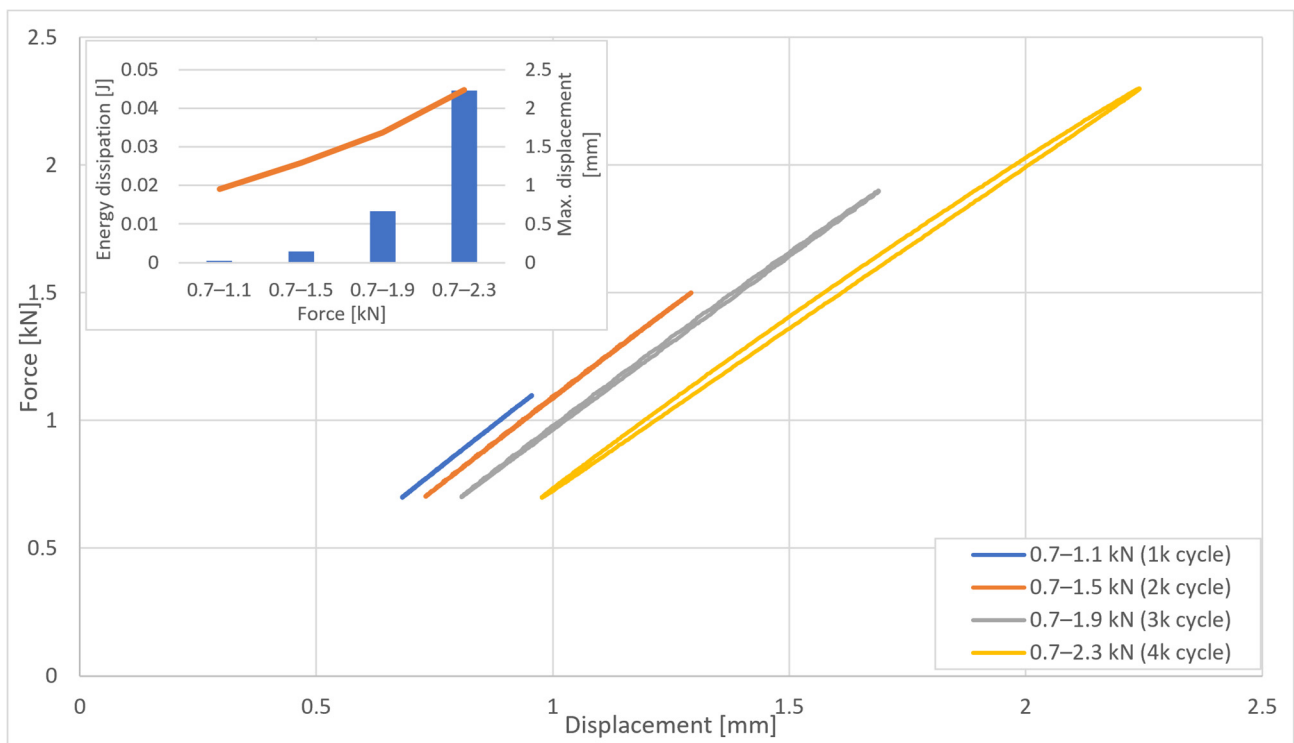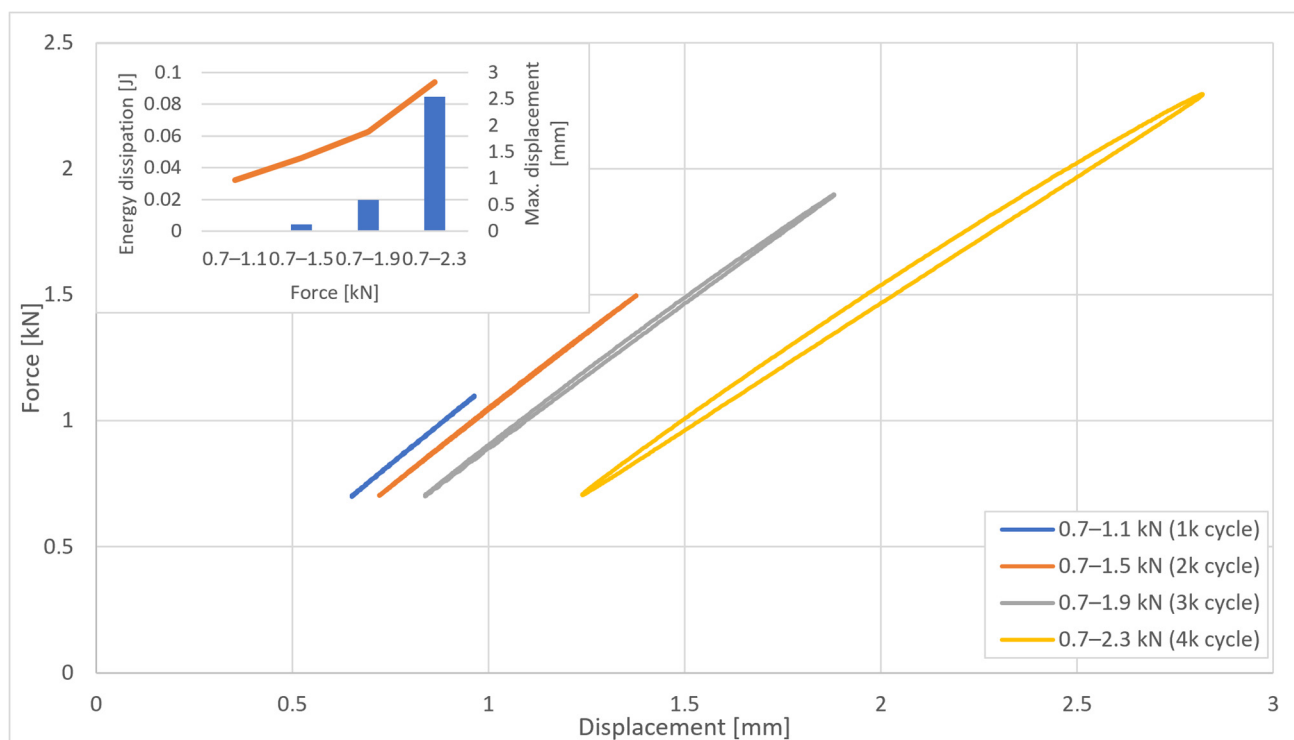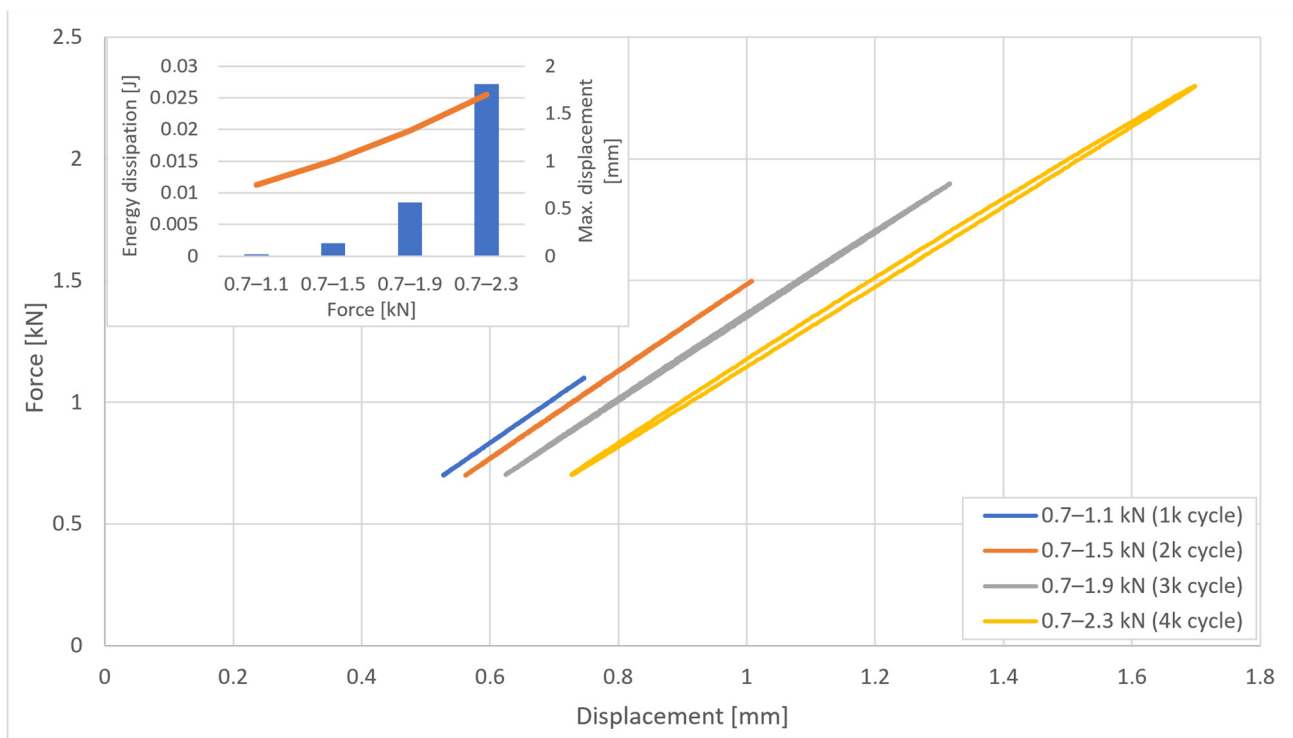

Figure 10. Change in maximum displacement and comparison of dissipation energy for increasing load blocks for neat bioPET.

Figure 11. Change in maximum displacement and comparison of dissipation energy for increasing load blocks for bioPET with the addition of 7.5% short basalt fibers.

Figure 12. Change in maximum displacement and comparison of dissipation energy for increasing load blocks for bioPET with the addition of 7.5% long basalt fibers.
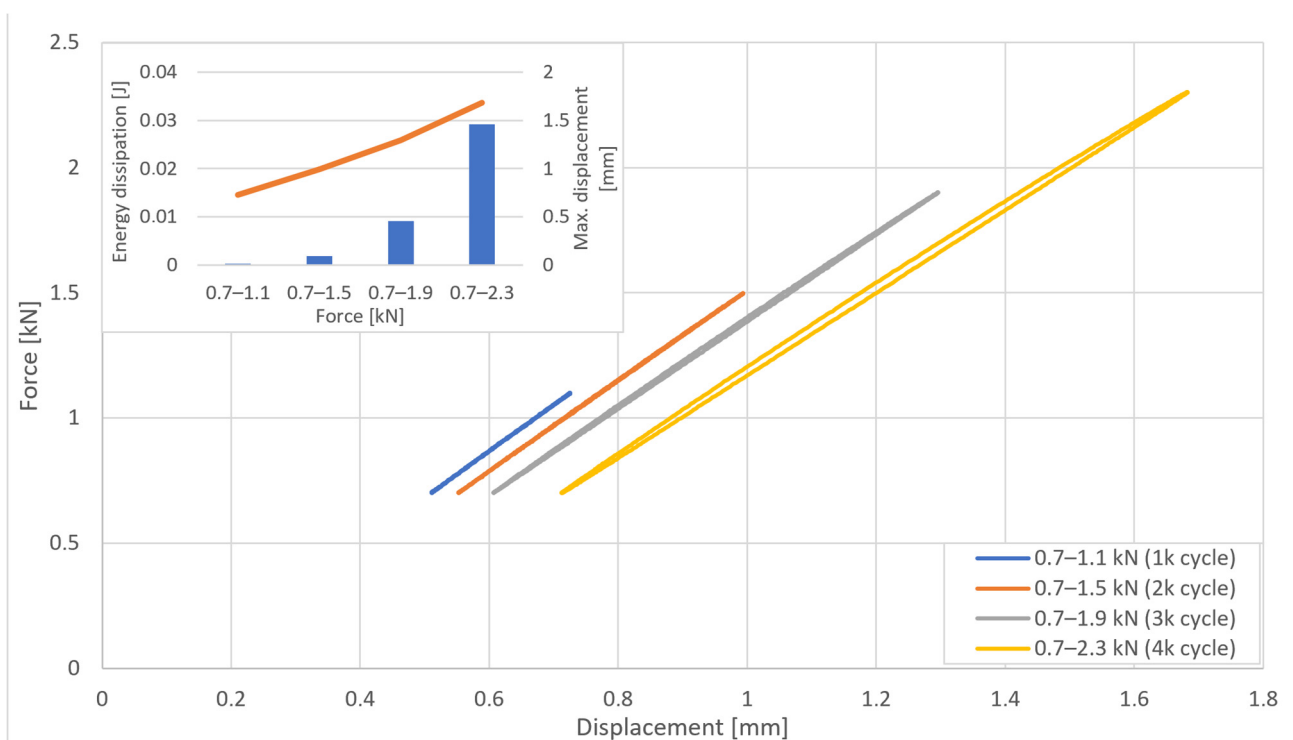
Figure 13. Change in maximum displacement and comparison of dissipation energy for increasing load blocks for bioPET with the addition of 15% short basalt fibers.

Figure 14. Change in maximum displacement and comparison of dissipation energy for increasing load blocks for bioPET with the addition of 15% long basalt fibers.

- bioPET

For neat bio-polyethylene terephthalate, we observe a low ability to disperse mechanical energy and rapid depletion of elastic load carrying capacity, which leads to rapid failure of the material at its yield point at a strain of 1.75%.

- bioPET + 7.5 SB
- bioPET + 7.5 LB

Comparing the compositions of 7.5 basalt fibers in the bioPET matrix, we see that the long fibers show a higher dynamic creep capacity (higher maximum displacements) and a twofold lower ability to dissipate mechanical energy, which allows them to achieve higher stiffness and strength.

- bioPET + 15 SB
- bioPET + 15 LB

A comparison of composites with 15% basalt fibers in the bioPET matrix shows that with an increased amount of fibers, the dynamic creep capacity is reduced and remains at a similar level, while the mechanical energy dissipation capacity remains lower with the short fibers.

Max. displacement
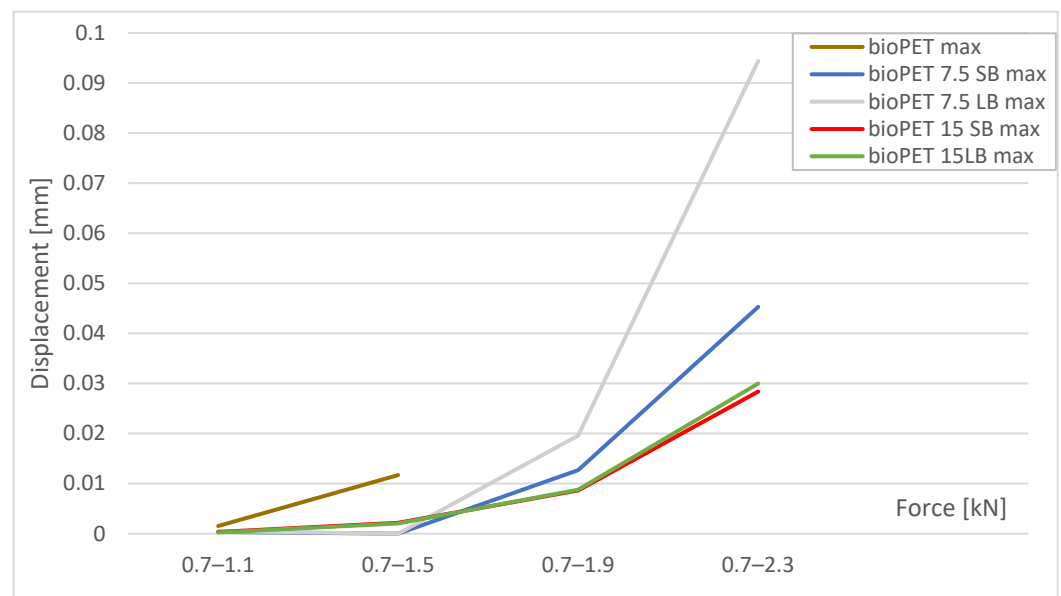
Figure 15. Comparison of the maximum displacement in increasing mechanical hysteresis blocks for bioPET and its composites.

A comparison of the increase in maximum displacement for each thousandth loop of mechanical hysteresis for all types of composites tested indicates a small value of permanent fatigue strength. For neat bioPET, there is a rapid increase in maximum displacement from the first loops. At the same time, we note for the composites the possibility of improving this strength by adding short fibers, especially in an amount of at least 15%.

The addition of fibers increases the ability to handle cyclic loads by lowering the composite's ability to dissipate mechanical energy and generate heat, reducing the internal friction forces present in the neat non-fiber-reinforced polymer. Under high-cycle dynamic loads, it is observed that as fatigue progresses, short fibers exhibit a reduced capacity for dynamic creep and uncontrolled increases in deformation, leading to failure.

3.2.4. Contact Angle and Total Surface Free Energy by the Owens–Wendt Method

Table 3 summarizes the results for contact angles measured with water and diiodomethane and total surface free energy using the Owens–Wendt method.

Table 3. Comparison of contact angle and total surface free energy in bioPET composites.

Sample	Contact Angle θ in Degrees		Total Surface Free Energy [mJ/m^2]
	Water	**Diiodomethane**	
bioPET	$85.7^{\pm 4.5}$	$28.6^{\pm 0.5}$	$46.0^{\pm 2.1}$
bPET + 7.5 SB	$76.5^{\pm 1.6}$	$45.4^{\pm 2.6}$	$42.2^{\pm 1.9}$
bPET + 7.5 LB	$85.7^{\pm 1.4}$	$35.4^{\pm 3.3}$	$43.2^{\pm 2.8}$
bPET+ 15 SB	$88.3^{\pm 3.8}$	$33.0^{\pm 2.0}$	$43.9^{\pm 4.2}$
bPET+ 15 LB	$79.6^{\pm 1.7}$	$42.7^{\pm 2.7}$	$42.1^{\pm 1.2}$

Neat bioPET is characterized by moderate hydrophobicity and a low contact angle, indicating a higher surface energy towards non-polar liquids. All basalt fiber-modified samples show a reduction in total surface free energy compared to neat bioPET, with the most significant reductions observed in bPET + 7.5 SB and bPET + 15 LB.

The addition of fibers appears to change the surface properties of bioPET, affecting its interaction with both polar and non-polar substances.

4. Conclusions

Injection molding was used to produce bioPET-based composites with the addition of two different lengths of basalt fibers. Analyzing the strength properties values from static tensile and three-point bending tests, it can be seen that the addition of basalt fibers significantly increases the tensile and flexural strengths and the modulus of elasticity, and significantly reduces the strain at break. The higher the basalt fiber content, the higher the values of these parameters. Composites containing short basalt fibers show a higher impact strength by about 15% compared to composites with long basalt fibers at the same fiber mass content. The addition of basalt fibers increased tensile strength by 26–41% and Young's modulus by 78–147%, causing almost 20 times less strain at break. Short fibers reinforce bioPET composites better than long fibers. For the same fiber amount, we can note that short fibers, relative to long fibers, result in an increase in tensile parameters by about 10% and bending parameters by 8–15%. Under high-cycle dynamic loads, it is observed that as fatigue progresses, short fibers exhibit a reduced capacity for dynamic creep and uncontrolled increases in deformation, leading to failure. The addition of basalt fibers alters the surface properties of bioPET composites. The modified composites show reduced total surface free energy and altered hydrophobicity. Utilizing basalt fibers, which are derived from natural sources, aligns with the goals of developing sustainable and eco-friendly materials. The research supports the potential for these composites to reduce the reliance on petroleum-based polymers and contribute to environmental conservation efforts.

Author Contributions: Conceptualization, S.K. and K.R.-Ż.; methodology, S.K. and K.R.-Ż.; validation, S.K.; formal analysis, K.R.-Ż.; investigation, K.R.-Ż. and S.K.; resources, K.R.-Ż.; data curation K.R.-Ż.; writing—original draft preparation S.K. and K.R.-Ż.; writing—review and editing K.R.-Ż.; visualization, K.R.-Ż.; supervision, S.K; funding acquisition, S.K. All authors have read and agreed to the published version of the manuscript.

Data Availability Statement: The datasets used and/or analyzed during the current study available from the corresponding author on request.

Conflicts of Interest: The authors declare no conflicts of interest.

References

1. Zhu, Y.; Romain, C.; Williams, C. Sustainable polymers from renewable resources. *Nature* **2016**, *540*, 354–362. [CrossRef] [PubMed]
2. Siracusa, V.; Blanco, I. Bio-Polyethylene (Bio-PE), Bio-Polypropylene (Bio-PP) and Bio-Poly(ethylene terephthalate) (Bio-PET): Recent Developments in Bio-Based Polymers Analogous to Petroleum-Derived Ones for Packaging and Engineering Applications. *Polymers* **2020**, *12*, 1641. [CrossRef] [PubMed]
3. Kwon, E.E.; Lee, J. Polyethylene terephthalate production from a carbon neutral resource. *J. Clean. Prod.* **2024**, *469*, 143210. [CrossRef]
4. Zheng, J.; Suh, S. Strategies to reduce the global carbon footprint of plastics. *Nat. Clim. Chang.* **2019**, *9*, 374–378. [CrossRef]
5. Hillmyer, M.A. The promise of plastics from plants. *Science* **2017**, *358*, 868–870. [CrossRef]
6. Spierling, S.; Knüpffer, E.; Behnsen, H.; Mudersbach, M.; Krieg, H.; Springer, S.; Albrecht, S.; Herrmann, C.; Endres, H.J. Bio-based plastics—A review of environmental, social and economic impact assessments. *J. Clean. Prod.* **2018**, *185*, 476–491. [CrossRef]
7. Abbood, I.S.; Odaa, S.A.; Hasan, K.F.; Jasim, M.A. Properties evaluation of fiber reinforced polymers and their constituent materials used in structures—A review. *Mater. Today Proc.* **2021**, *43 Pt 2*, 1003–1008. [CrossRef]
8. Gupta, M.K.; Srivastava, R.K. Mechanical Properties of Hybrid Fibres Reinforced Polymer Composite: A Review. *Polym.-Plast. Technol. Eng.* **2015**, *55*, 626–642. [CrossRef]
9. Rajak, D.K.; Pagar, D.D.; Menezes, P.L.; Linul, E. Fiber-Reinforced Polymer Composites: Manufacturing, Properties, and Applications. *Polymers* **2019**, *11*, 1667. [CrossRef]
10. Prashanth, S.; Subbaya, K.M.; Nithin, K.; Sachhidananda, S. Fiber reinforced composites—A review. *J. Mater. Sci. Eng* **2017**, *6*, 2–6.
11. Mittal, G.; Rhee, K.Y.; Mišković-Stanković, V.; Hui, D. Reinforcements in multi-scale polymer composites: Processing, properties, and applications. *Compos. Part B Eng.* **2018**, *138*, 122–139. [CrossRef]
12. Li, Z.; Ma, J.; Ma, H.; Xu, X. Properties and Applications of Basalt Fiber and Its Composites. *IOP Conf. Ser. Earth Environ. Sci.* **2018**, *186*, 012052. [CrossRef]
13. Militký, J.; Mishra, R.; Jamshaid, H. 20—Basalt fibers. In *Handbook of Properties of Textile and Technical Fibres*, 2nd ed.; Woodhead Publishing: Sawston, UK, 2018; pp. 805–840. ISBN 9780081012727. [CrossRef]
14. Jamshaid, H.; Mishra, R. A green material from rock: Basalt fiber—A review. *J. Text. Inst.* **2015**, *107*, 923–937. [CrossRef]
15. Dhand, V.; Mittal, G.; Rhee, K.Y.; Park, S.-J.; Hui, D. A short review on basalt fiber reinforced polymer composites. *Compos. Part B Eng.* **2015**, *73*, 166–180. [CrossRef]
16. Tavadi, A.R.; Naik, Y.; Kumaresan, K.; Jamadar, N.I.; Rajaravi, C. Basalt fiber and its composite manufacturing and applications: An overview. *Int. J. Eng. Sci. Technol.* **2021**, *13*, 50–56. [CrossRef]
17. Pareek, K.; Saha, P. Basalt Fiber and Its Composites: An Overview. In Proceedings of the National Conference on Advances in Structural Technologies (CoAST-2019), Silchar, India, 1–3 February 2019.
18. Singha, K. A short review on basalt fiber. *Int. J. Text. Sci.* **2012**, *1*, 19–28.
19. Liu, J.; Chen, M.; Yang, J.; Wu, Z. Study on Mechanical Properties of Basalt Fibers Superior to E-glass Fibers. *J. Nat. Fibers* **2020**, *19*, 882–894. [CrossRef]
20. Kessler, E.; Gadow, R.; Straub, J. Basalt, glass and carbon fibers and their fiber reinforced polymer composites under thermal and mechanical load. *AIMS Mater. Sci.* **2016**, *3*, 1561–1576. [CrossRef]
21. King, F.L. Basalt Fiber: An Ancient Material for Innovative and Modern Application. *Middle East J. Sci. Res.* **2014**, *22*, 308–312. [CrossRef]
22. Wu, G.; Wang, X.; Wu, Z.; Dong, Z.; Zhang, G. Durability of basalt fibers and composites in corrosive environments. *J. Compos. Mater.* **2015**, *49*, 873–887. [CrossRef]
23. Amaro, A.; Pinto, D.; Bernardo, L.; Lopes, S. Basalt Fibers used as Reinforcing Materials in Different Polymers—A Review. In Proceedings of the Fourth International Conference on Innovative Natural Fibre Composites for Industrial Applications, Rome, Italy, 17–18 October 2013.
24. Kumbhar, V.P. An overview: Basalt rock fibers-new construction material. *Acta Eng. Int.* **2014**, *2*, 11–18.
25. Ronkay, F.; Czigány, T. Development of composites with recycled PET matrix. *Polym. Adv. Technol.* **2006**, *17*, 830–834. [CrossRef]
26. Cheng, X.; Liu, J.; Han, C.; Zhang, X.; Wu, Z. Silane coupling agent impact on surface features of modification of basalt fibers and the rheological properties of basalt fiber reinforced asphalt. *Constr. Build. Mater.* **2023**, *366*, 130182. [CrossRef]
27. Arslan, C.; Dogan, M. The effects of fiber silane modification on the mechanical performance of chopped basalt fiber/ABS composites. *J. Thermoplast. Compos. Mater.* **2020**, *33*, 1449–1465. [CrossRef]
28. Arslan, C.; Dogan, M. The effects of silane coupling agents on the mechanical properties of basalt fiber reinforced poly(butylene terephthalate) composites. *Compos. Part B Eng.* **2018**, *146*, 145–154. [CrossRef]
29. Kracalik, M.; Pospíšil, L.; Slouf, M.; Mikesova, J.; Sikora, A.; Šimoník, J.; Fortelný, I. Recycled poly(ethylene terephthalate) reinforced with basalt fibres: Rheology, structure, and utility properties. *Polym. Compos.* **2008**, *29*, 437–442. [CrossRef]

30. Ralph, C.; Lemoine, P.; Archer, E.; McIlhagger, A. Mechanical properties of short basalt fibre reinforced polypropylene and the effect of fibre sizing on adhesion. *Compos. Part B Eng.* **2019**, *176*, 107260. [CrossRef]

31. Maiti, S.; Islam, M.R.; Uddin, M.A.; Afroj, S.; Eichhorn, S.J.; Karim, N. Sustainable Fiber-Reinforced Composites: A Review. *Adv. Sustain. Syst.* **2022**, *6*, 2200258. [CrossRef]

32. Zhao, C.; Wang, Z.; Zhu, Z.; Guo, Q.; Wu, X.; Zhao, R. Research on different types of fiber reinforced concrete in recent years: An overview. *Constr. Build. Mater.* **2023**, *365*, 130075. [CrossRef]

33. Nawafleh, N.; Celik, E. Additive manufacturing of short fiber reinforced thermoset composites with unprecedented mechanical performance. *Addit. Manuf.* **2020**, *33*, 101109. [CrossRef]

34. Zhang, D.; He, M.; Qin, S.; Yu, J. Effect of fiber length and dispersion on properties of long glass fiber reinforced thermoplastic composites based on poly(butylene terephthalate). *RSC Adv.* **2017**, *7*, 15439–15454. [CrossRef]

35. Arslan, C.; Dogan, M. The mechanical and thermal properties of chopped basalt fiber-reinforced poly (butylene terephthalate) composites: Effect of fiber amount and length. *J. Compos. Mater.* **2019**, *53*, 2465–2475. [CrossRef]

36. Blackman, Z.; Olonisakin, K.; MacFarlane, H.; Rodriguez-Uribe, A.; Tripathi, N.; Mohanty, A.K.; Misra, M. Sustainable Basalt Fiber Reinforced Polyamide 6,6 Composites: Effects of Fiber Length and Fiber Content on Mechanical Performance. *Compos. Part C Open Access* **2024**, *14*, 100495. [CrossRef]

37. Amuthakkannan, P.; Manikandan, V.; Jappes, J.W.; Uthayakumar, M. Effect of fibre length and fibre content on mechanical properties of short basalt fibre reinforced polymer matrix composites. *Mater. Phys. Mech.* **2013**, *16*, 107–117.

38. *PN-EN ISO 3167:2004*; Plastics—Multipurpose Test Specimens. ISO: Geneva, Switzerland, 2014.

39. *PN-EN ISO 1183-1:2019-12*; Plastics—Determination of Density of Non-Foamed Plastics—Part 1: Immersion Method, Pycnometer Method and Displacement Method. ISO: Geneva, Switzerland, 2019.

40. *PN-EN ISO 527-1:2019-12*; Plastics—Determination of Tensile Properties—Part 1: General Principles. ISO: Geneva, Switzerland, 2019.

41. *PN-EN ISO 178:2019-10*; Plastics—Determination of Flexural Properties. ISO: Geneva, Switzerland, 2019.

42. *PN-EN ISO 179-1:2010*; Plastics—Determination of Charpy Impact Properties—Part 1: Non-Instrumented Impact Test. ISO: Geneva, Switzerland, 2010.

43. Rudawska, A.; Jacniacka, E. Analysis for determining surface free energy uncertainty by the Owen–Wendt method. *Int. J. Adhes. Adhes.* **2009**, *29*, 451–457. [CrossRef]

44. Żenkiewicz, M. Methods for the calculation of surface free energy of solids. *J. Achiev. Mater. Manuf. Eng.* **2007**, *24*, 137–145.